



Aalborg Universitet

AALBORG UNIVERSITY
DENMARK

Neural and muscular determinants of maximal rate of force development

Dideriksen, Jakob Lund; Del Vecchio, Alessandro; Farina, Dario

Published in:
Journal of Neurophysiology

DOI (link to publication from Publisher):
[10.1152/jn.00330.2019](https://doi.org/10.1152/jn.00330.2019)

Publication date:
2020

Document Version
Accepted author manuscript, peer reviewed version

[Link to publication from Aalborg University](#)

Citation for published version (APA):
Dideriksen, J. L., Del Vecchio, A., & Farina, D. (2020). Neural and muscular determinants of maximal rate of force development. *Journal of Neurophysiology*, 123(1), 149-157. <https://doi.org/10.1152/jn.00330.2019>

General rights

Copyright and moral rights for the publications made accessible in the public portal are retained by the authors and/or other copyright owners and it is a condition of accessing publications that users recognise and abide by the legal requirements associated with these rights.

- Users may download and print one copy of any publication from the public portal for the purpose of private study or research.
- You may not further distribute the material or use it for any profit-making activity or commercial gain
- You may freely distribute the URL identifying the publication in the public portal -

Take down policy

If you believe that this document breaches copyright please contact us at vbn@aub.aau.dk providing details, and we will remove access to the work immediately and investigate your claim.

NEURAL AND MUSCULAR DETERMINANTS OF MAXIMAL RATE OF FORCE DEVELOPMENT

Jakob L. Dideriksen¹, Alessandro Del Vecchio², Dario Farina²

1: Department of Health Science and Technology, Aalborg University, Aalborg, Denmark.

2: Department of Bioengineering, Imperial College London, London, UK

RUNNING HEAD: Neural and muscular determinants of ballistic force

CORRESPONDING AUTHOR:

Jakob L. Dideriksen (jldi@hst.aau.dk)

Fredrik Bajers Vej 7D, 9220 Aalborg Ø, Denmark.

ABSTRACT

The ability to produce rapid forces requires quick motor unit recruitment, high motor unit discharge rates, and fast motor unit force twitches. The relative importance of these parameters for maximum rate of force development (RFD), however, is poorly understood. In this study, we systematically investigated these relations using a computational model of motor unit pool activity and force. Across simulations, neural and muscular properties were systematically varied in experimentally observed ranges. Motor units were recruited over an interval starting from contraction onset (range: 22-233 ms). Upon recruitment, discharge rates declined from an initial rate (range: 89-212 pps) with varying likelihood of doublet (inter-spike interval of 3 ms; range: 0-50%). Finally, muscular adaptations were modeled by changing average twitch contraction time (range: 42-78 ms). Spectral analysis showed that the effective neural drive to the simulated muscle had smaller bandwidths than the average motor unit twitch indicating that the bandwidth of the motor output, and thus the capacity for explosive force, was limited mainly by neural properties. The simulated RFD increased by $1,050 \pm 281$ %MVC/s from the longest to the shortest recruitment interval. This effect was >4-fold higher than the effect of increasing the initial discharge rate, >5-fold higher than the effect of increasing the chance of doublets, and >6-fold higher than the effect of decreasing twitch contraction times. The simulated results suggest that the physiological variation of the rate by which motor units are recruited during ballistic contractions is the main determinant for the variability in RFD across individuals.

NEW & NOTEWORTHY

An important limit of human performance is the ability to generate explosive movements by means of rapid development of muscle force. The physiological determinants of this ability, however, are poorly understood. In this study we show using extensive simulations that the rate by which motor units are recruited is the main limiting factor for maximum rate of force development.

KEYWORDS: Rate of force development, motor unit, computational model.

INTRODUCTION

The motor output is determined by the neural activation of the muscle (rate coding and recruitment of the motor neuron pool) and the contractile properties of the motor units (the dynamics of the force twitches). This implies that the characteristics of these parameters constrain the limits of muscle performance. One of these performance limits is the ability to generate explosive force, usually characterized as the maximal rate of force development (RFD). To achieve maximal RFD, high motor unit discharge rates, rapid recruitment of the motor unit pool, and effective summation of motor unit twitches are required. For example, the initial motor unit discharge rates during ballistic contractions are substantially higher than in slower contractions (Desmedt and Godaux, 1977a; Del Vecchio et al., 2019b) and increase following prolonged training with ballistic contraction (Van Cutsem et al., 1998). This increase may, at least in part, reflect a higher number of so-called doublets (two discharges with very short inter-spike interval) (Van Cutsem et al., 1998; Christie and Kamen, 2006; Mrówczyński et al., 2015). Furthermore, the force produced during electrically-induced contractions when all motor units are recruited concurrently increases by a higher rate than during ballistic voluntary contractions (de Ruyter et al., 2004; Folland et al., 2014) when motor units are recruited gradually according to size (Desmedt and Godaux, 1977a, 1977b). Finally, muscles with high proportion of fast twitch motor units exhibit the highest RFD (Desmedt and Godaux, 1978) and prolonged training with ballistic contractions involves shortening of the average twitch contraction time (Gruber et al., 2007). Although the neural and contractile factors influencing rate of force development have been discussed previously (Duchateau and Baudry, 2014; Folland et al., 2014; Del Vecchio et al., 2019b), their relative importance is not known.

Recently, we showed that the variance in human RFD is associated to the maximal motor unit discharge rate and to the latency from the recruitment of the first to the last motor unit (recruitment interval) (Del Vecchio et al., 2019b). However, it was not possible to evaluate the relative importance of the neural and contractile parameters on RFD due to the unknown variance in motor unit twitches among subjects. For this reason, here we aimed to investigate the neural and muscular determinants of maximal RFD using a realistic computational model of a ballistic isometric contraction to a stable near-maximal contraction level. This model allowed systematic variations of the motor unit discharge rate (including the chance for occurrence of doublets), the rate by which motor units were recruited (determining the time interval until full recruitment), and the motor unit twitch contraction times. The ranges of values assigned to these parameters were derived from our recent experimental study (Del Vecchio et al., 2019b), as well as previously published experimental findings.

The simulation results were analyzed in two complementary ways. First, the neural and muscular properties were analyzed in the frequency-domain and their bandwidths were compared. This analysis was based on the notion that motor unit force can be described as the convolution between the motor neuron spike train and

the motor unit twitch force. Thus, the power spectrum of the force generated by each motor unit is the product of the power spectrum of the spike train and the square magnitude of the Fourier transform of the twitch force. Similarly, the power spectrum of the total force can be approximated as the product of the power spectrum of the neural drive to the muscle (sum of all motor unit spike trains) and the square module of the average motor unit twitch force (average force twitch response over all active motor units). In this way, the average motor unit twitch can be regarded as a filter for the neural drive and the characteristics of the motor output is determined by this filtered neural drive. The power of the filtered neural drive determines the magnitude of the force, while its bandwidth reflects the speed of the force: The larger the bandwidth, the greater the ability to produce rapid forces. If the neural drive contains high frequencies, but these are filtered out by the twitch, the twitch would be the limiting factor for the output. Thereby the muscular properties would be the main determinant for RFD, and vice versa. In the second part of the analysis, the RFD was calculated for all combinations of values assigned to the main model parameters. This enabled direct comparison of the degree to which each parameter affected RFD. The outcome of both analyses showed that the main determinant of maximal RFD was the rate by which motor units were recruited.

METHODS

Experimental data

The experimental data was adopted from a previous study (Del Vecchio et al., 2019b). In that study, 20 men (age: 24.9 ± 3 yr, weight: 75.4 ± 8.6 kg, height: 180 ± 10 cm) performed isometric ankle-dorsiflexion explosive force contractions. Participants were instructed to contract as fast and as forceful as possible and then hold force at levels above 75% of the maximum force. The force signals were recorded concurrently with high-density surface electromyography, which was decomposed into individual motor unit contributions. On average, 12.1 ± 5.7 motor units were decomposed per contraction. Across all subjects, the motor units initially exhibited a few discharges with very short inter-spike interval (as low as 4.7 ms) after which the discharge rate declined steadily over a period of 200-300 ms. This behavior is compatible with discharge patterns observed in previous studies (Granit et al., 1963; Desmedt and Godaux, 1977a; Van Cutsem et al., 1998). After this period, a steady discharge rate was observed (mean: 37 ± 8 pulses per second; pps). Figure 1 summarizes the relevant data from the experiment. Across the 20 subjects, the average initial discharge rate and ranged between 89 and 212 pulses per second (pps; mean: 132 ± 31 pps; Fig. 1A). Within each subject, the initial discharge rate did not depend on the recruitment threshold. The recruitment interval ranged between 22 to 117 ms (mean: 60 ± 28 ms; Fig. 1B). The RFD was expressed in units % of MVC/s. RFD ranged from 350 to 654 %MVC/s (mean: 442 ± 85 %MVC/s) (Fig. 1C).

Computational model

Motor unit spike trains were based on a predefined function describing the discharge rate. This function contained a linear decrease from the assigned initial discharge rate (see *Simulations*) to 37 pps over a period of 250 ms (Del Vecchio et al., 2019b). After this period, the discharge rate remained constant. This template was applied to all motor units of the pool, but noise was added individually for each motor unit to ensure a coefficient of variation for the inter-spike interval of approximately 10% (Matthews, 1996; Moritz et al., 2005). In addition, the model included simulation of doublets by additional discharges 3 ms after a predefined percentage (see *Simulations*) of randomly selected simulated discharges.

The smallest motor unit was recruited at the onset of the contraction and the recruitment time of the other motor units was exponentially distributed throughout the assigned recruitment interval (see *Simulations*). In this way, most motor units were recruited in the first period of the recruitment interval, whereas the largest motor units were recruited at the end, as previously observed (Desmedt and Godaux, 1977a).

The isometric force was simulated from the discharge patterns based on a modified version of the model proposed by Fuglevand et al. (Fuglevand et al., 1993). Since this model reflected the first dorsal interosseous, the model was adapted to reflect the tibialis anterior muscle. This involved setting the number of motor units to 188 (Xiong et al., 2008). Furthermore, the proportion of type II muscle fibers in the first dorsal interosseous is approximately 50% (Fuglevand et al., 1993; Enoka and Fuglevand, 2001) while it is 30% in the tibialis anterior (Henriksson-Larsén et al., 1983). By replacing Eq. 15 in (Fuglevand et al., 1993) by a linear distribution from 90 to 30 ms, the proportion of muscle fibers with contraction times <35 ms was reduced from 50% to 30%. The smallest motor unit was assigned the highest contraction time. As in the original version of the model, there was a 100-fold range of twitch amplitudes across the motor unit pool, since this range is compatible with experimental data for the tibialis anterior (Van Cutsem et al., 1998).

Next, a more detailed model for the non-linear gain of the twitch amplitudes was implemented. During trains of action potentials, the amplitude of the motor unit twitch increases with respect to the first twitch, with a factor that depends on the interval between the action potentials (Burke et al., 1976). In the original version of the model, this gain was modeled based on experimental observations of the twitch after more than three action potentials. This gain, however, depends on the inter-spike interval in a different way for the second and third action potential (Burke et al., 1976). Whereas this difference has a small influence on simulations of sustained contractions, which was the primary focus of the original model (Fuglevand et al., 1993), it may have a substantial impact on simulations of ballistic contractions involving a small number of discharged action potentials. Consequently, the twitch gain (G) was modeled as a function of the inter-spike interval (ISI) normalized to the twitch contraction time (CT) as follows:

$$G = 0.84 \frac{ISI^3}{CT} - 3.08 \frac{ISI^2}{CT} + 1.16 \frac{ISI}{CT} + 4.33, \text{ for } AP\# = 2$$

$$G = 1.14 \frac{ISI^3}{CT} - 5.84 \frac{ISI^2}{CT} + 7.23 \frac{ISI}{CT} + 1.19, \text{ for } AP\# = 3$$

$$G = 1.29 \frac{ISI^3}{CT} - 6.91 \frac{ISI^2}{CT} + 9.82 \frac{ISI}{CT} - 0.89, \text{ for } AP\# \geq 4$$

Where AP# denotes the action potential number. The gain was limited to values >1 and was set to 1 for normalized inter-spike intervals >2.3. Figure 2 illustrates these relations along with the experimentally observed values (Burke et al., 1976). R² between the simulated parameters and the experimental values was 0.97, 0.92, and 0.97 for the second, third, and fourth action potential, respectively.

Simulations

Across the simulations, the discharge rate was varied either by changing the initial discharge rate or by increasing the chance of doublets. In the first set of simulations, three different values were assigned to the initial discharge rate (minimum, median and maximum experimentally observed values: 89, 132, 212 pps; Fig. 1A). In each simulation, one of these rates were assigned uniformly to all motor units. In these simulations the chance of doublets was set to 0%. In another set of simulations, the chance of doublets was set to 0%, 25%, or 50%. Again, in each simulation, this rate applied to all motor units. At 50%, on average every 2nd discharge assigned a doublet (an additional discharge after 3 ms), which is equivalent to the rate of inter-spike intervals <5 ms observed for the first few discharges after 12 weeks of explosive training (Van Cutsem et al., 1998). Although it is not clear if this chance of doublets occurring remains stable throughout the rest of the explosive contraction, this rate was imposed on the entire simulation since doublets have also been observed in sub-maximal steady contractions (Kudina and Andreeva, 2010). In simulations varying the chance of doublets, the initial discharge rate (discounting doublets) was set to 132 pps.

Five values were assigned to the recruitment interval distributed in 8 evenly spaced intervals between 22 ms (lowest experimentally observed value; Fig. 1B) and 233 ms. The upper bound of this range (233 ms) was set to twice the highest value experimentally observed by EMG decomposition (Del Vecchio et al., 2019b). This choice was motivated by the fact that EMG decomposition provides a relatively small sample of the active motor units and therefore it is unlikely that the first and/or the last recruited motor units are identified in EMG decomposition studies. This leads to an underestimate of the recruitment interval. Accordingly, pilot simulations showed that the slowest experimentally observed RFD (<400 %MVC/s; Fig. 1C) could only be obtained in simulations with recruitment intervals longer than the maximal value previously observed in the experiments. Furthermore, three gains were applied to the motor unit twitch contraction times (CT-gain): 0.7 (fast motor units; average contraction time: 42 ms), 1 (normal motor units representing the expected values for tibialis anterior; average contraction time: 60 ms), and 1.3 (slow motor units; average contraction time: 78 ms). This range of gains was selected to reflect the largest adaptations in contraction time observed

following different types of resistance training (Schmidtbleicher and Haralambie, 1981; Pääsuke et al., 1999; Gruber et al., 2007; Jenkins et al., 2016). To summarize, the ranges described above for the model parameters represent the entire realistic range of values for the three parameters.

The ballistic force was simulated using every combination of these parameters (total of 150 different combinations) and each of these simulations was repeated six times. The duration of each simulation was 500 ms, since a peak in the rate of force development was achieved earlier than 500 ms into the contraction across all settings. For each simulated ballistic force, the RFD was calculated in the same way as for the experimental data (unit: %MVC/s). The MVC was estimated individually for each CT-gain as the average force produced during a 3-s simulation (excluding the first second) with the discharge rate for all motor units set to 60 pps (Enoka and Fuglevand, 2001).

The cut-off frequencies of the neural drive (sum of spike trains from all motor units) and the average twitch (weighted by twitch amplitudes) were estimated from their power spectra as the frequency at which the power had decreased by 50% with respect to the maximal power equivalent to decline of 3 dB.

RESULTS

Figure 3 shows examples of the neural drive (smoothed cumulative spike train) and the average motor unit twitch force in the time and frequency domain from simulations with different settings. The power spectra were derived from the interval that reflected the RFD (the period from 0% of MVC to the maximum RFD). In the simulation with relatively long recruitment interval (172 ms) and median initial discharge rate (132 pps) (black unbroken line in Fig. 3A), the magnitude of the neural drive (density of motor unit action potentials) peaked approximately 88 ms after the onset of the contraction (time=0). The decrease in neural drive after the peak reflected the gradual decrease in discharge rate to approximately 37 pps. Increasing the initial discharge rate for the motor units (212 pps; black dashed line) implied a higher peak magnitude of the neural drive, but no substantial difference in time to peak (83 ms after contraction onset). Consequently, the cut-off frequencies of the power spectra of the neural drives in these conditions were similar (2.1 Hz for both low and high initial discharge rate, respectively; black unbroken and dashed lines, Fig. 3B). This implies that although an increase in the initial discharge rate involved increased power of low-frequency neural drive components, it does not lead to large improvements in the ability to produce rapid force. Introducing a 50% chance of doublets (grey unbroken line, Fig. 3A and 3B) had almost the same effect as increasing the discharge rate to 212 pps in the time and frequency domain. Since a 50% chance of doublets is equivalent to an effective discharge rate 198 pps, this indicates that the neural drive is determined by the net number of discharges and not their specific timing. In other words, the same changes in the neural drive can be obtained by increasing the average discharge rate or by increasing the chance of doublets. Contrary to the impact of

rate coding on the power spectrum of the neural drive, the cut-off frequency of the neural drive increased substantially (4.3 Hz) when the recruitment interval was reduced (22 ms; grey dashed lines in Fig. 3A and 3B). This implied an increase in the ability to support rapid force generation. Therefore, changes in rate coding affected the bandwidth of the neural drive to a smaller extent than the rate of recruitment.

The duration of the compound motor unit twitch (Fig. 3C) influenced the muscle cut-off frequency (Fig. 3D). With a slow twitch (CT-gain: 1.3; light grey lines in Fig. 3C and 3D) the cut-off frequency was 4.3 Hz. The muscle cut-off frequency increased to 4.7 Hz (CT-gain: 1; dark grey lines in Fig. 3C and 3D) and 5.1 Hz (CT-gain: 0.7; black lines in Fig. 3C and 3D) when changing the CT-gain. This implied, as expected, that a fast compound twitch provided the best support for high-frequency force output.

The representative power spectra shown in Figure 3B and 3D illustrates that, although there was some overlap in the ranges of the cut-off frequencies for the neural drive and the compound motor unit twitch, these frequencies tended to be higher for the compound motor unit twitch. These tendencies are confirmed when analyzing all simulations, where the compound motor unit twitch cut-off frequency was on average 0.54 ± 0.33 Hz higher than the cut-off frequency for the neural drive. This suggests that the neural drive (in particular the recruitment interval) in most conditions is the main determinant of the ability of a muscle to generate rapid force or, alternatively, that the speed of muscle contraction can be boosted by a more rapid drive. The effect of a rapid drive is further enhanced when the motor unit twitches are fast (i.e. when the average motor unit twitch cut-off frequency is high), since in this case the filtering effect of the twitch on the neural drive is minimal and there is a greater margin for an increase in rapidity of the neural drive to impact force speed.

Figure 4 shows the ballistic force in two representative simulation conditions. In the first condition (Fig. 4A, 4C, 4E), the muscle had a normal range of twitch contraction speeds across the motor units (CT gain = 1) but a fast motor neuron pool (i.e. high initial discharge rate and short recruitment interval). With these settings, RFD was 1,045 %MVC/s. In the second condition (Fig. 4B, 4D, 4F), the muscle had a faster twitch contraction speeds (CT gain = 0.7) but a slower motor neuron pool (i.e., low initial discharge rate and high recruitment interval). With these settings the simulated RFD was reduced by approximately 50% in the second compared to the first condition. This suggests that increasing the motor unit twitch contraction speed by 30% was far from sufficient to compensate for the impact of the slower behavior of the motor neuron pool. This tendency is confirmed when considering all simulation settings (Fig. 5 and 6). In Figure 5, RFD is shown as a function of the recruitment interval for each assigned value for the initial discharge rate (lines in each panel) and for each CT gain (Fig. 5A, 5B, and 5C, respectively). In the simulations shown in Figure 5, the chance of doublets was set to 0%. Overall, RFD was most strongly related to the recruitment interval. Specifically, increasing the recruitment interval from the longest to the shortest simulated value (234 ms to 22 ms) implied, on average, an increase in RFD of $1,050 \pm 281$ %MVC/s. This increase was 252 ± 59 %

expressed as a relative change. In comparison, an increase in initial discharge rate from lowest to highest rate (89 pps to 212 pps) implied an average increase in RFD of 250 ± 136 %MVC/s, equivalent to 36 ± 13 %, while decreasing the CT-gain (thereby increasing the contraction times) from 1.3 to 0.7 implied an average increase in RFD of 158 ± 149 %MVC/s, equivalent to 20 ± 11 %. The strength of the relation between recruitment interval and RFD was affected by the twitch contraction times, as predicted from the spectral analysis of the neural drive and the compound motor unit twitch (Fig. 3). Specifically, in simulations with a fast muscle (CT-gain=0.7), the difference in average RFD between the shortest and longest recruitment interval (1,641 %MVC/s) was larger than with a slow muscle (CT-gain=1.3; 1,163 %MVC/s).

Considering the simulations in which the chance of doublets were varied (Fig. 6) the recruitment range remained the main determinant of RFD. Increase this chance from 0% to 50% implied an average increase in RFD of 205 ± 67 %MVC/s, equivalent to 29 ± 5 %. As indicated in Figure 3, the increase in RFD caused by a higher chance of doublets was largely equivalent to increasing the discharge rate by an equivalent number of action potentials per second.

DISCUSSION

In this study, we systematically investigated the impact of rate coding, recruitment, and contractile properties of a motor unit pool on the maximal RFD during ballistic isometric contractions to a stable near-maximal contraction level. Although all three parameters affected RFD, the rate by which motor units were recruited had the highest impact within the range of simulated values. This observation was confirmed by the spectral analysis of the neural drive and the average muscle twitch force, which showed that the main limiting factor for high-frequency content of the force was indeed motor unit recruitment interval (Fig. 3). Specifically, this implies that the largest improvement in RFD can be achieved by minimizing the recruitment interval within the range of experimentally observed values (Fig. 1).

The simulation approach applied in this study cannot reveal whether adaptations in the recruitment interval actually occur in natural conditions. The results, however, suggest that the experimentally observed improvement in RFD following prolonged training of up to 48% (Gruber et al., 2007) likely involved some reduction in the time to full motor unit recruitment, since neither realistic adaptations in twitch contraction time nor changes in rate coding (by means of initial discharge rates or chance of doublets) generated changes in RFD of that magnitude in the simulations (Fig. 5, 6). Indeed, we recently showed indirectly that the increase in RFD in chronically strength/power trained athletes seem to be dependent on a decrease in motor unit recruitment interval before the onset of force (Del Vecchio et al., 2018). Furthermore, it is likely that an increase in initial discharge rate and a higher recruitment rate both can be achieved by an increased magnitude of excitatory synaptic input to the motor neuron pool. Accordingly, a linear relation between the

maximal discharge rate of motor neurons and the rate at which motor units are recruited has been shown (Del Vecchio et al., 2019b). In this way, the experimentally observed increase in initial discharge rate after training (Van Cutsem et al., 1998) was likely accompanied by faster motor unit recruitment. It is also possible, although it cannot be fully proved from the results shown, that higher initial discharge rates occurred as an epiphenomenon of neural adaptations aiming to increase RFD by reducing the recruitment interval. The recruitment interval, however, is difficult to estimate experimentally, since in principle it requires complete decomposition of the motor neuron pool, which is not possible with current methods (McGill et al., 2005; Negro et al., 2016). This is underlined by the experimental data adopted for this study, where an average of 12 motor units was decomposed per contraction. Although this is a relatively high number compared to many previous single motor unit studies, it likely represents less than 10% of the motor unit pool (Xiong et al., 2008). Accordingly, the results indicated that the experimentally observed recruitment intervals (Fig. 1B) to some degree underestimated the real interval, since the simulated RFD at, e.g., the average experimentally observed recruitment interval (60 ms; Fig. 1B) were higher ($>800\%$ MVC/s; Fig. 5) than those observed experimentally ($<650\%$ MVC/s; Fig. 1C). To some degree, this uncertainty implies that it is unclear if the full range of simulated values for the recruitment interval (22-232 ms) realistically reflects natural variations across subjects. This uncertainty and the fact that the relative difference between the lowest and highest value of this range of recruitment interval values was higher than for the other parameters implies that the outcome may to some degree overestimate the relative importance of this parameter. However, since variations in recruitment interval had on average >4 times stronger impact on RFD compared to the other parameters, the duration of the recruitment interval would remain the main determinant of RFD even if the natural range for this parameter is somewhat smaller than simulated. For example, if the range of simulated values for the recruitment interval was reduced by 50% (range: 83-173 ms), the average relative change in RFD ($65 \pm 11\%$) would still be substantially higher than for the other parameters (Fig. 5).

Several previous studies have discussed the neural and muscular determinants of RFD (Duchateau and Baudry, 2014; Folland et al., 2014; Del Vecchio et al., 2019a, 2019b). Duchateau & Baudry argued that the maximal RFD is constrained mainly by the initial motor unit discharge rate, in part based on simulations using a similar model as in this study (Duchateau and Baudry, 2014). Although our results indicate some influence of initial discharge rate and chance of doublets on RFD, it was not identified as the primary determinant. In their simulations, however, only the force generated by four action potentials per motor unit were considered (Duchateau and Baudry, 2014). Since discharge rates are expected to decline rapidly after the first action potentials (Sawczuk et al., 1995; Miles et al., 2005), it is likely that the interval from the onset of the contraction until maximal RFD contain more than four discharges per motor unit. For example, in the simulation illustrated in Fig. 4D and 4F, motor unit #1 exhibited 12 action potentials before maximum RFD was achieved. This implies that considering such low numbers of action potentials (i.e., selecting only those

action potentials with low inter-spike interval) may lead to an overestimation of the impact of discharge rate with respect to natural conditions. Furthermore, these previous simulations focused on RFD for single motor unit force and therefore did not reflect the impact of the gradual recruitment of motor units over a certain time interval. Another factor that serves to decrease the impact of initial discharge and chance of doublets on RFD is the non-linear twitch gain illustrated in Fig. 2. These relations imply that for the fastest motor units, a decrease in the discharge rate below 100 pps increases twitch force amplitude, which will to some degree counteract the decrease in twitch summation at lower rates. Finally, Duchateau & Baudry also argued against an impact of changes in contractile properties on RFD. The data underlying this argument, however, was based on the spike-triggered averaging technique (Van Cutsem et al., 1998), which has recently been shown to be highly inaccurate (Dideriksen and Negro, 2018). In another study, Folland and colleagues found that the relative importance of neural and muscular properties changed throughout the time course of the ballistic contraction using an experimental approach (Folland et al., 2014). Here, the neural properties were estimated by the amplitude of the surface electromyographic signal (EMG). The EMG signal, however, cannot differentiate between rate coding and recruitment, which implies that although the study demonstrated that both muscular and neural properties affect maximal RFD, it did not allow for a direct quantification of the impact of properties such as discharge rate, recruitment rate and twitch contraction time. Finally, Del Vecchio and colleagues found that recruitment interval as well as maximal discharge rate predicted maximal RFD (Del Vecchio et al., 2019a, 2019b). To summarize, our study confirms the findings of these previous studies, but extends them by quantifying the relation between each of the three parameters and RFD allowing direct identification of the main determinant for maximal RFD.

The simulation approach used in this study has limitations that should be acknowledged. First, the amplitude of the simulated motor unit twitches was not varied across simulations although this has been observed following prolonged resistance training (Van Cutsem et al., 1998; Pääsuke et al., 1999). Adaptations in the twitch amplitude may reflect muscle hypertrophy (Charette et al., 1991; Seynnes et al., 2007) and/or a more efficient transfer of muscle force to the bones (and thus the force transducer) via stiffer tendons (Kubo et al., 2001; Bojsen-Møller et al., 2005; Waugh et al., 2013). Such adaptations increase the effective force producing capacity of the muscle and thereby also RFD when expressed in absolute units (N/s). However, when considering normalized forces as in the current study, a change in the absolute force producing capacity across simulations would not affect the results. A second limitation is that the same discharge rate profiles (uniform initial discharge rate, same rate of discharge rate decline) were assigned to all motor units. In sustained contractions, the peak discharge rate depends on motor unit recruitment threshold (Fuglevand et al., 1993; Barry et al., 2007), but this dependency has not been observed during brief ballistic contractions (Del Vecchio et al., 2019b). It cannot, however, be ruled out that the behavior of the decomposed motor units underlying this study (Fig. 1) may not be representative for the entire motor unit pool, since decomposition based on surface EMG may be more sensitive to superficial units, which have a higher composition of type II

units in the tibialis anterior (Henriksson-Larsén et al., 1983). Regarding the decline in discharge rate, it is believed to reflect mainly intrinsic motor neuron properties (Sawczuk et al., 1995; Miles et al., 2005). Nevertheless, it is possible that the synaptic input to motor neurons recruited at the late phase of the ballistic contraction (unlike those recruited from the onset of the contraction) is affected by feedback from muscle afferents (e.g. muscle spindles or Golgi tendon organs) due to the electromechanical delay and nerve conduction times. However, even if systematic variations in discharge rates across the motor unit pool would occur, it will likely have a relatively small effect on RFD (Fig. 5). A third limitation is that the model reflected only one muscle, whereas the force produced by natural joints reflects the activity from synergistic agonist muscles as well as antagonist muscles. However, it has been shown that antagonist muscle activity has little effect on RFD in practice (Folland et al., 2014). Finally, it should be noted that the findings of the study are based on a computational model which reflects a simplified representation of the current understanding of neuromechanical behavior. Consequently, if future experiments invalidate any of the assumption underlying the model, the conclusions of this study should be reconsidered accordingly. Nevertheless, the simulation results are in agreement with previous experimental findings (Del Vecchio et al., 2018), as discussed above.

In conclusion, we used a simulation approach to identify the determinants of the ability of muscles to generate rapid force. Although motor unit discharge rates and contractile properties to some degree affected simulated RFD, the interval between recruitment of the first and the last motor unit had the largest impact on this rate. This suggests that the variation in the rate by which motor units are recruited during ballistic contractions across individuals is the main determinant for maximal RFD.

REFERENCES

- Barry BK, Pascoe MA, Jesunathadas M, Enoka RM.** Rate coding is compressed but variability is unaltered for motor units in a hand muscle of old adults. *J Neurophysiol* 97: 3206–3218, 2007.
- Bojsen-Møller J, Magnusson SP, Rasmussen LR, Kjaer M, Aagaard P.** Muscle performance during maximal isometric and dynamic contractions is influenced by the stiffness of the tendinous structures. *J Appl Physiol* 99: 986–994, 2005.
- Burke RE, Rudomin P, Zajac FE.** The effect of activation history on tension production by individual muscle units. *Brain Res* 109: 515–529, 1976.
- Charette SL, McEvoy L, Pyka G, Snow-Harter C, Guido D, Wiswell RA, Marcus R.** Muscle hypertrophy response to resistance training in older women. *J Appl Physiol* 70: 1912–1916, 1991.

367 **Christie A, Kamen G.** Doublet Discharges in Motoneurons of Young and Older Adults. *J Neurophysiol* 95:
368 2787–2795, 2006.

369 **Van Cutsem M, Duchateau J, Hainaut K.** Changes in single motor unit behaviour contribute to the
370 increase in contraction speed after dynamic training in humans. *J Physiol* 513 (Pt 1: 295–305, 1998.

371 **Desmedt JE, Godaux E.** Ballistic contractions in man: characteristic recruitment pattern of single motor
372 units of the tibialis anterior muscle. *J Physiol* 264: 673–693, 1977a.

373 **Desmedt JE, Godaux E.** Fast motor units are not preferentially activated in rapid voluntary contractions in
374 man. *Nature* 267: 717–719, 1977b.

375 **Desmedt JE, Godaux E.** Ballistic contractions in fast or slow human muscles; discharge patterns of single
376 motor units. *J Physiol* 285: 185–196, 1978.

377 **Dideriksen JL, Negro F.** Spike-triggered averaging provides inaccurate estimates of motor unit twitch
378 properties under optimal conditions. *J Electromyogr Kinesiol* 43: 104–110, 2018.

379 **Duchateau J, Baudry S.** Maximal discharge rate of motor units determine the maximal rate of force
380 development during ballistic contractions in human. *Front Hum Neurosci* 8, 2014.

381 **Enoka RM, Fuglevand AJ.** Motor unit physiology: some unresolved issues. *Muscle Nerve* 24: 4–17, 2001.

382 **Folland JP, Buckthorpe MW, Hannah R.** Human capacity for explosive force production: Neural and
383 contractile determinants. *Scand J Med Sci Sport* 24: 894–906, 2014.

384 **Fuglevand AJ, Winter DA, Patla AE.** Models of recruitment and rate coding organization in motor-unit
385 pools. *J Neurophysiol* 70: 2470–2488, 1993.

386 **Granit R, Kernell D, Shortess GK.** Quantitative aspects of repetitive firing of mammalian motoneurons,
387 caused by injected currents. *J Physiol* 168: 911–931, 1963.

388 **Gruber M, Gruber SBH, Taube W, Schubert M, Beck SC, Gollhofer A.** Differential effects of ballistic
389 versus sensorimotor training on rate of force development and neural activation in humans. *J Strength Cond*
390 *Res* 21: 274–282, 2007.

391 **Henriksson-Larsén KB, Lexell J, Sjöström M.** Distribution of different fibre types in human skeletal
392 muscles. I. Method for the preparation and analysis of cross-sections of whole tibialis anterior. *Histochem J*
393 15: 167–178, 1983.

394 **Jenkins NDM, Housh TJ, Buckner SL, Bergstrom HC, Smith CM, Cochrane KC, Hill EC, Miramonti**

395 **AA, Schmidt RJ, Johnson GO, Cramer JT.** Four weeks of high- versus low-load resistance training to
 396 failure on the rate of torque development, electromechanical delay, and contractile twitch properties. *J*
 397 *Musculoskelet Neuronal Interact* 16: 135–144, 2016.

398 **Kubo K, Kanehisa H, Fukunaga T.** Effects of different duration isometric contractions on tendon elasticity
 399 in human quadriceps muscles. *J Physiol* 536: 649–655, 2001.

400 **Kudina LP, Andreeva RE.** Repetitive doublet firing of motor units: Evidence for plateau potentials in
 401 human motoneurons? *Exp Brain Res* 204: 79–90, 2010.

402 **Matthews PB.** Relationship of firing intervals of human motor units to the trajectory of post-spike after-
 403 hyperpolarization and synaptic noise. *J Physiol* 492: 597–628, 1996.

404 **McGill KC, Lateva ZC, Marateb HR.** EMGLAB: An interactive EMG decomposition program. *J Neurosci*
 405 *Methods* 149: 121–133, 2005.

406 **Miles GB, Dai Y, Brownstone RM.** Mechanisms underlying the early phase of spike frequency adaptation
 407 in mouse spinal motoneurons. *J Physiol* 566: 519–532, 2005.

408 **Moritz CT, Barry BK, Pascoe MA, Enoka RM.** Discharge rate variability influences the variation in force
 409 fluctuations across the working range of a hand muscle. *J Neurophysiol* 93: 2449–2459, 2005.

410 **Mrówczyński W, Celichowski J, Raikova R, Krutki P.** Physiological consequences of doublet discharges
 411 on motoneuronal firing and motor unit force. *Front Cell Neurosci* 9, 2015.

412 **Negro F, Muceli S, Castronovo AM, Holobar A, Farina D.** Multi-channel intramuscular and surface EMG
 413 decomposition by convolutive blind source separation. *J Neural Eng* 13, 2016.

414 **Pääsuke M, Ereline J, Gapeyeva H.** Twitch contractile properties of planter flexor muscles in power and
 415 endurance trained athletes. *Eur J Appl Physiol Occup Physiol* 80: 448–451, 1999.

416 **de Ruiters CJ, Kooistra RD, Paalman MI, de Haan A.** Initial phase of maximal voluntary and electrically
 417 stimulated knee extension torque development at different knee angles. *J Appl Physiol* 97: 1693–1701, 2004.

418 **Sawczuk A, Powers RK, Binder MD.** Spike frequency adaptation studied in hypoglossal motoneurons of
 419 the rat. *J Neurophysiol* 73: 1799–1810, 1995.

420 **Schmidtbleicher D, Haralambie G.** Changes in contractile properties of muscle after strength training in
 421 man. *Eur J Appl Physiol Occup Physiol* 46: 221–228, 1981.

422 **Seynnes OR, de Boer M, Narici M V.** Early skeletal muscle hypertrophy and architectural changes in

response to high-intensity resistance training. *J Appl Physiol* 102: 368–373, 2007.

Del Vecchio A, Falla D, Felici F, Farina D. The relative strength of common synaptic input to motor neurons is not a determinant of the maximal rate of force development in humans. *J Appl Physiol* 127: 205–214, 2019a.

Del Vecchio A, Negro F, Falla D, Bazzucchi I, Farina D, Felici F. Higher muscle fiber conduction velocity and early rate of torque development in chronically strength trained individuals. *J Appl Physiol* 125: 1218–1226, 2018.

Del Vecchio A, Negro F, Holobar A, Casolo A, Folland JP, Felici F, Farina D. You are as fast as your motor neurons: speed of recruitment and maximal discharge of motor neurons determine the maximal rate of force development in humans. *J. Physiol.* (2019b). doi: 10.1113/JP277396.

Waugh CM, Korff T, Fath F, Blazevich AJ. Rapid force production in children and adults: Mechanical and neural contributions. *Med Sci Sports Exerc* 45: 762–771, 2013.

Xiong GX, Zhang JW, Hong Y, Guan Y, Guan H. Motor unit number estimation of the tibialis anterior muscle in spinal cord injury. *Spinal Cord* 46: 696–702, 2008.

FIGURE CAPTIONS

Figure 1: Distribution of experimentally observed values for initial discharge rate (A), recruitment interval (B), and time to reach 80% MVC (C) across 20 subjects. This data was adopted from (Del Vecchio et al., 2019b).

Figure 2: The non-linear gain of the 2nd (black line), 3rd (dark grey line) and 4th-nth twitch during summation of overlapping twitches as a function of the inter-spike interval (ISI) normalized to the contraction time (CT). Symbols indicate the experimental data reported by Burke et al. 1976. The two additional x-axes indicate the relation between the twitch gains and the non-normalized discharge rate for a slow-twitch motor unit (contraction time: 90 ms) and a fast-twitch motor unit (contraction time: 30 ms).

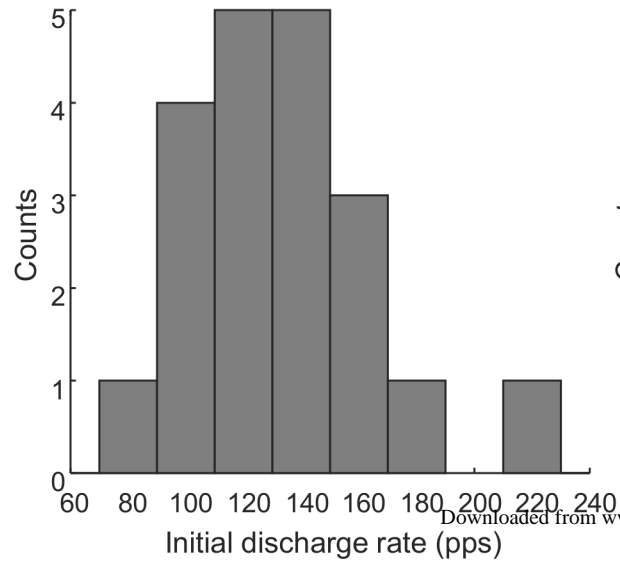
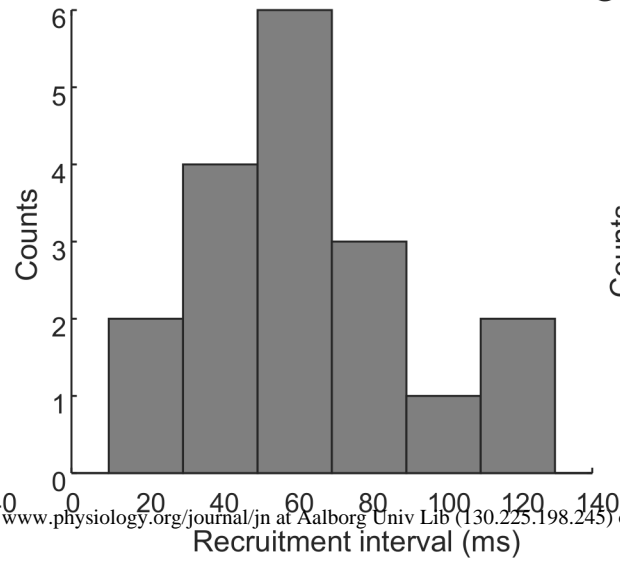
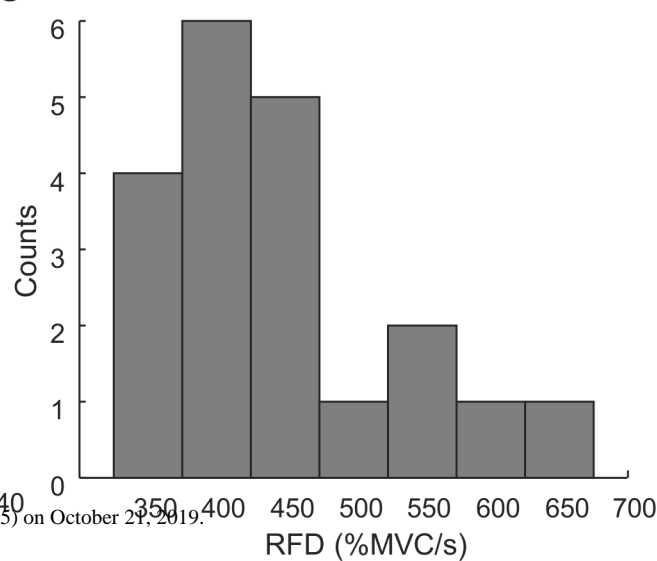
Figure 3: Time (A) and frequency (B) domain representations of the neural drive in four different simulation conditions with different initial discharge rates (IDR), recruitment intervals (RI) and/or chance of doublets (DC). The neural drives depicted in A were the smoothed cumulative spike trains (40 ms hamming window). In this way, the rate indicated on the y-axis represents the rate of action potentials across the motor unit pool. The power spectra of the neural drive were derived from the interval from the onset of the contraction until the simulated force reached the point of maximal RFD. For all four simulations in panels A

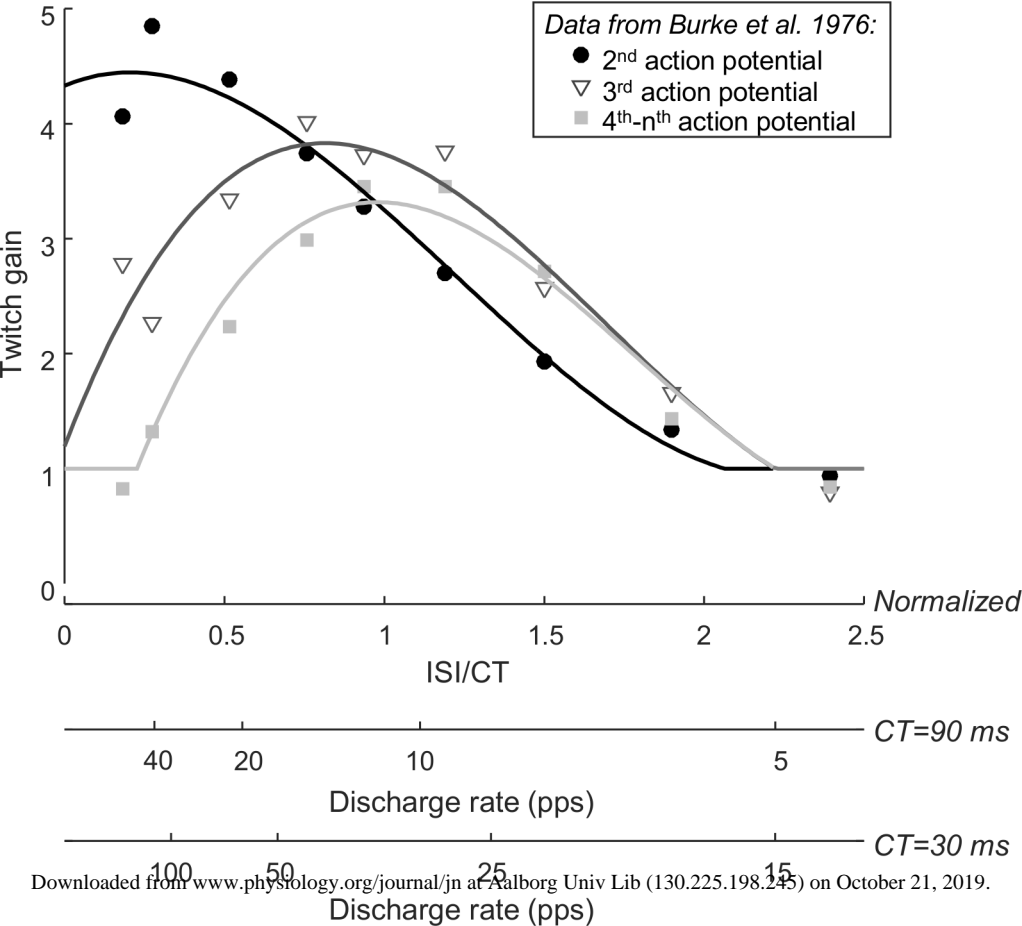
and B the CT gain was 1. In B, the circles indicate the cut-off frequency. Time (C) and frequency (D) domain representations of the cumulative motor unit twitch during three different simulation conditions: CT gain = 1.3 (slow muscle); CT gain = 1 (normal muscle); CT gain = 0.7 (fast muscle). The power spectra of the cumulative motor unit twitches were derived from the interval equivalent to the time it took for the simulated force to reach the point of maximal RFD. For all three simulations the initial discharge rate was 132 pps, the recruitment interval was 82 ms and the chance of doublets was 0%. In D, the circles indicate the cut-off frequency.

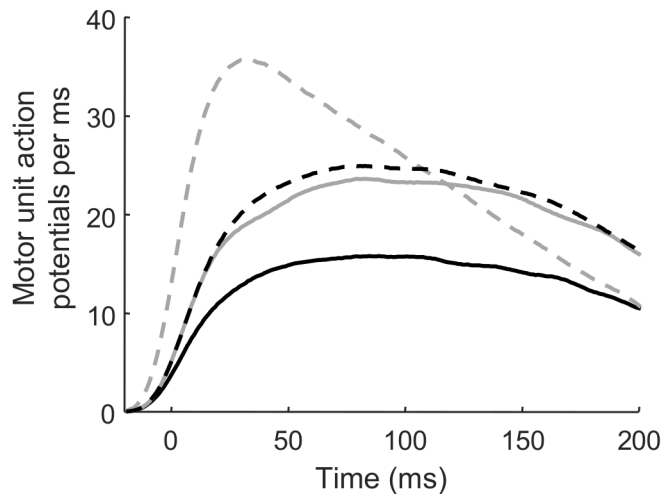
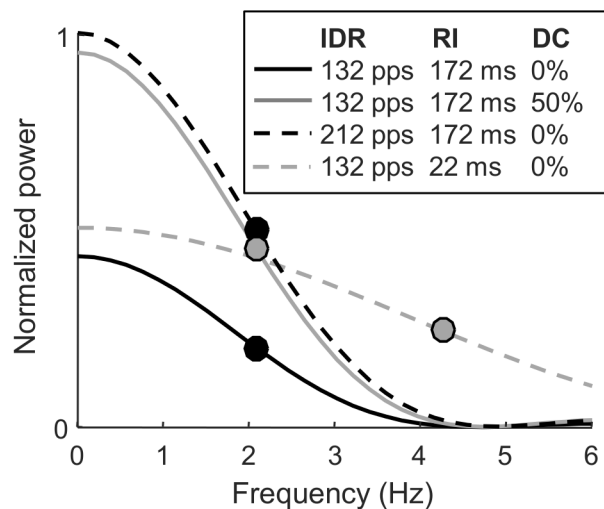
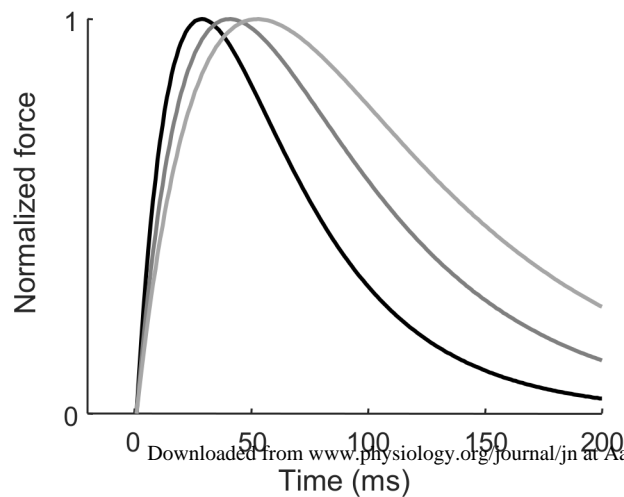
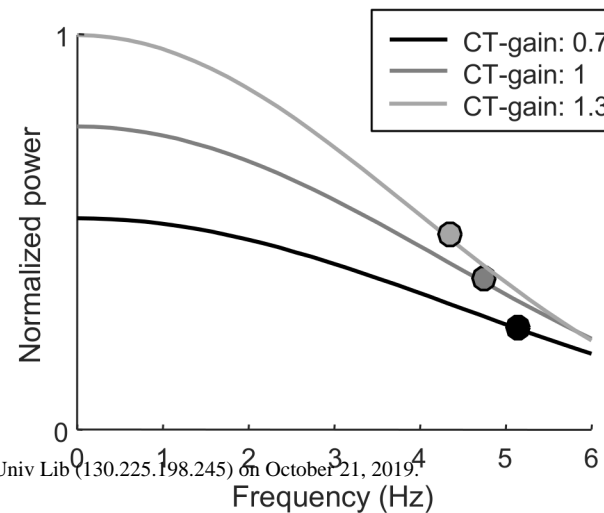
Figure 4: Two representative simulations illustrating the effects of the muscular and neural model parameters on the rate of force development. Panels A and B show the distribution of contraction times across the motor unit pool. Panels C and D show the motor unit discharge patterns for the smallest (#1) and largest (#188) motor unit. Here, each symbol indicates the instantaneous discharge rate of one motor unit during the first 250 ms of the contraction. Panels E and F show the simulated forces. The left column represents a model with a normal muscle (motor unit contraction times between 30 and 90 ms) and a fast motor neuron pool (relatively high initial discharge rate (IDR) and short recruitment interval), while the right column represents the opposite: a model with a fast muscle and a relatively slow motor unit pool. In both simulations, the chance of doublets was set to 0%.

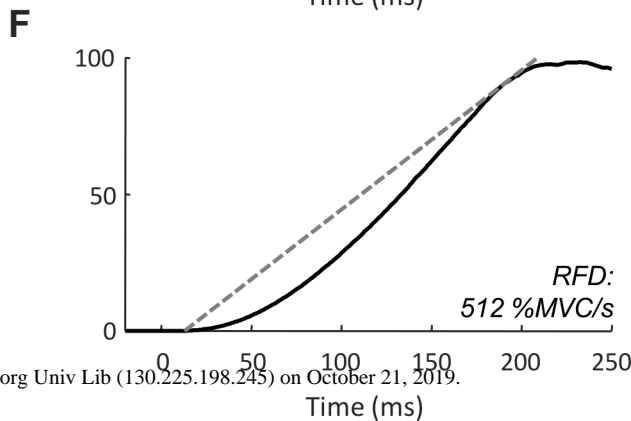
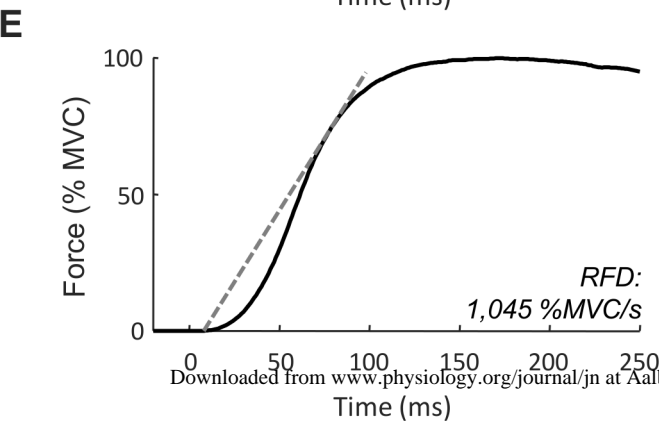
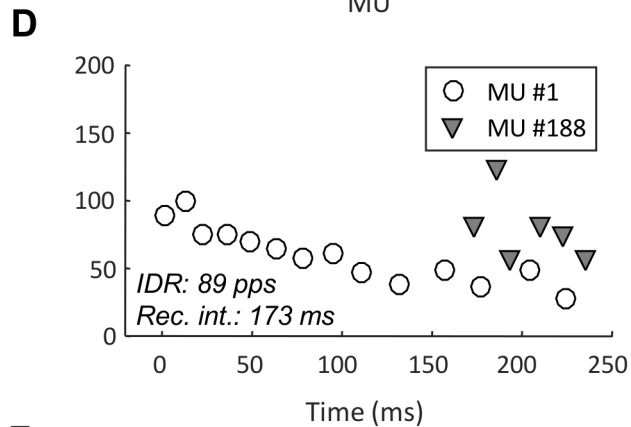
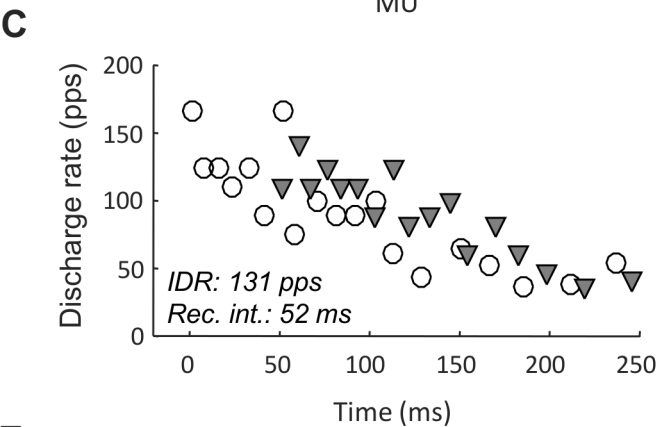
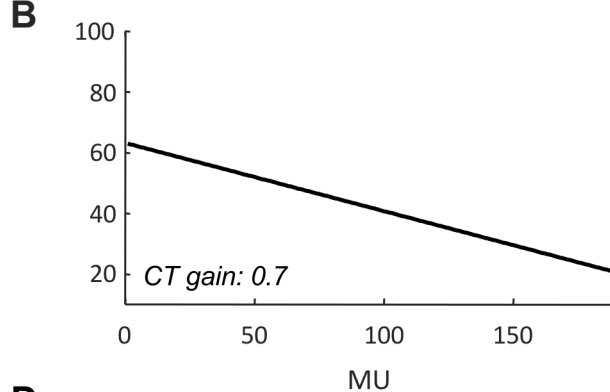
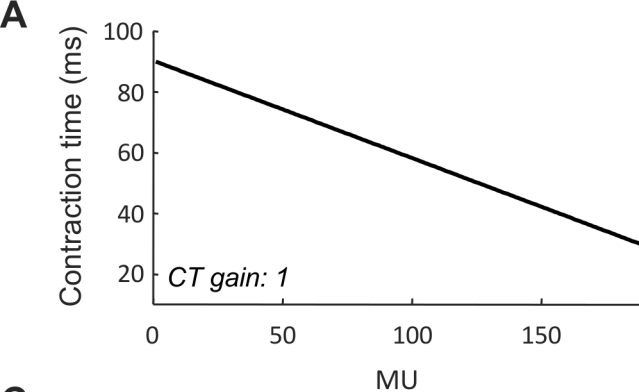
Figure 5: Average RFD as a function of recruitment interval for all initial discharge rates and for all contraction time gains in simulations with 0% chance of doublets. Panel A represents contraction time gain of 0.7 (fastest muscle), panel B represents contraction time gain of 1 (normal muscle), and panel C represents contraction time gain of 1.3 (slow muscle). The lines in each panel represent simulations with different initial motor unit discharge rates.

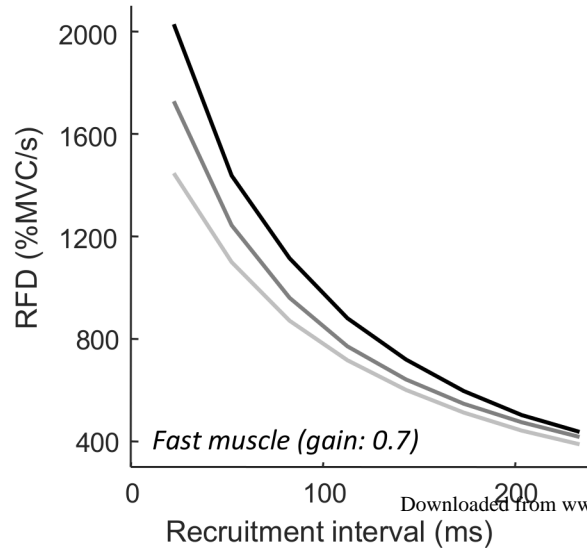
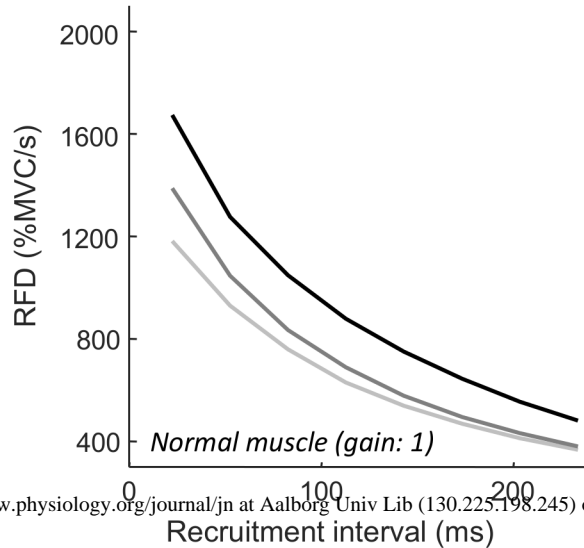
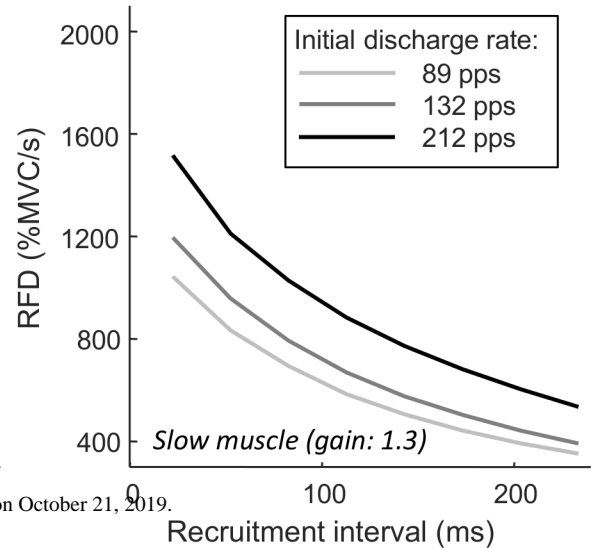
Figure 6: Average RFD as a function of recruitment interval for across all percentages assigned to the change of doublets occurring and for all contraction time gains in simulations with initial discharge rates of 132 pps. Panel A represents contraction time gain of 0.7 (fastest muscle), panel B represents contraction time gain of 1 (normal muscle), and panel C represents contraction time gain of 1.3 (slow muscle). The lines in each panel represent simulations with different chances of doublets.

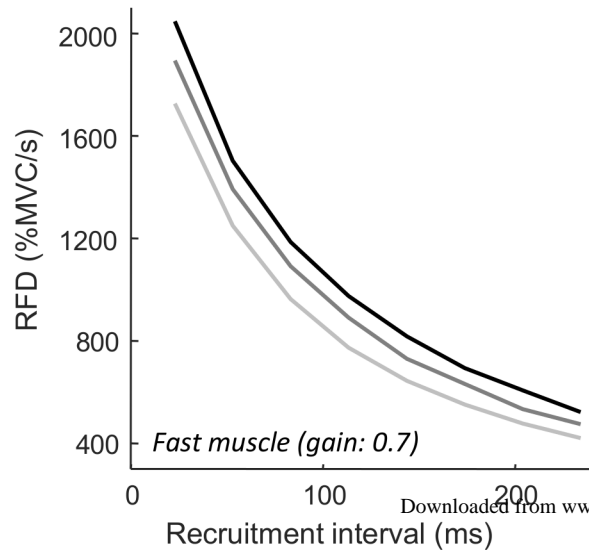
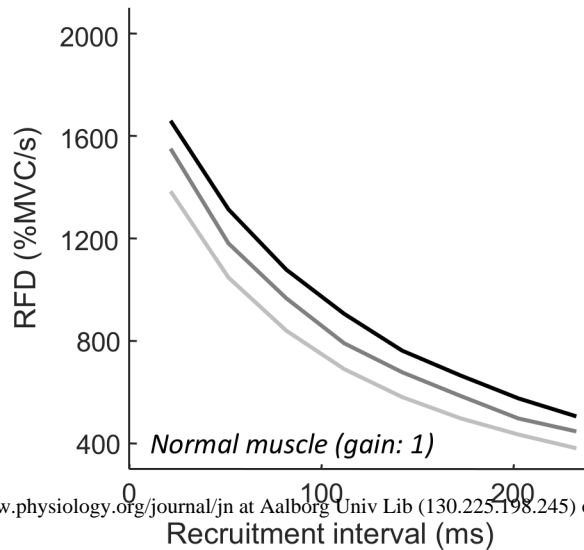
A**B****C**



A**B****C****D**



A**B****C**

A**B****C**